# Material Basis and Mechanism for Anti-tumor Efficacy of *Isodon suzhouensis* Roots Based on UPLC-Q-TOF-MS/MS and Network Pharmacology

**Meihui DUAN[1,2], Meiqi WEI[1,2], Weixian YANG[1,2], Weiqing ZHANG[2], Xianji LIU[2], Chen YAN[2]**

1. Guizhou University of Traditional Chinese Medicine, Guiyang 550025, China; 2. People's Hospital of Anshun City, Anshun 561000, China

**Abstract** [**Objectives**] This study was conducted to explore the anti-tumor substances and mechanism of *Isodon suzhouensis* roots based on high performance liquid chromatography-quadrupole-time-of-flight mass spectrometry (UPLC-Q-TOF-MS), network pharmacology and molecular docking verification. [**Methods**] Main chemical composition information in *I. suzhouensis* roots was confirmed based on UPLC-Q-TOF-MS/MS, literature and databases. The targets of active components in *I. suzhouensis* roots were predicted by Swiss Target Prediction database. Relevant targets of cancer were obtained from GeneCards, OMIM, and TTD databases. The intersecting targets of drug active component targets and disease targets were obtained using Venn diagram, and a protein-protein interaction network (PPI) was constructed by using STRING database. GO enrichment analysis and KEGG pathway analysis were carried out through the Metascape database. An "active component-antitumor targets-enrichment pathway" network was constructed with the Cytoscape software. Molecular docking was used for preliminary verification. [**Results**] A total of 58 compounds were identified from the roots of *I. suzhouensis*, showing 55 antitumor active components and 202 potential targets. Network pharmacology analysis showed that *I. suzhouensis* roots might acted on AKT1, TP53, ALB, GAPDH, CTNNB1, SRC and other core targets through dehydrodiisoeugenol, tetramethylcurcumin, isosteviol, ursonic acid, echinocystic acid, oleanonic acid and other active compounds, regulating pathways in cancer, PI3K/Akt, lipid and atherosclerosis, prostate cancer, proteoglycans in cancer, AGE-RAGE and other pathways, thus exerting antitumor effects. The results of molecular docking verification showed that the antitumor components of *I. suzhouensis* roots had strong binding activity with disease target proteins. [**Conclusions**] The effective components of *I. suzhouensis* roots can exert antitumor effects through multiple components, multiple targets and multiple pathways, providing a scientific and reasonable theoretical basis for subsequent research.

**Key words** *Isodon suzhouensis* roots; Antitumor effect; UPLC-Q-TOF-MS/MS; Network pharmacology; Molecular docking

**DOI**:10.19759/j.cnki.2164-4993.2024.06.016

According to the statistics of cancer incidence and mortality in China regularly reported by the National Cancer Center (NCC), 4 824 700 new cancer cases and 2 574 200 new cancer deaths occurred in China in 2022, while lung cancer, liver cancer, stomach cancer, colorectal cancer and esophageal cancer were the five major causes of cancer deaths, accounting for 67.50% of the total cancer deaths[1]. The issue of tumor diseases is urgent. At present, in addition to adhering to the guidelines of the Healthy China Action Plan and the cancer prevention and control action plan, we should also actively look for new drugs with antitumor effects. In recent years, traditional Chinese medicine has provided many new ideas in the clinical treatment of tumor diseases because of its advantages of multiple components, multiple targets and multiple pathways.

*Isodon suzhouensis*, a plant in *Isodon* of Labiatae, is a traditional Chinese herbal medicine widely distributed in many provinces in central and southern China, as well as one of the well-known specialty plants in Suzhou, Anhui Province[2]. Because of its low toxicity and no side effects, it is also a rare medicinal and edible plant in this genus, and the whole herb can be used as medicine. Its traditional efficacy suggests that it has the functions of clearing away heat and toxic materials, promoting blood circulation and removing blood stasis[2], and modern pharmacology shows that it has antitumor[3], anti-inflammation[4], bacteriostatic[5], and immunity-improving effects, so *I. suzhouensis* is also called "natural plant antibiotic"[6]. Existing scientific research results show that many pure active components, including wangzaozin A, glaucocalyxin A, and oleanolic acid, have been extracted and separated from *I. suzhouensis* for further research, and it is speculated that they may be the main components of *I. suzhouensis* for its antibacterial, anti-inflammatory and anticancer effects[3,4,7-9].

In modern pharmacology, Kim B and Gan P found that glaucocalyxin A and glaucocalyxin B can reduce the production of BV-2 cells through tumor necrosis factors such as TNF (tumor necrosis factor)-α, COX (cyclooxygenase)-2 and iNOS (inducible nitric oxide synthase), and inhibit the expression of protein nuclear factor kB(NF-kB) and heme oxygenase 1(HO-1) in BV-2 cells, thereby protecting cells[10-11]. Through *in-vitro* cell experiments, Shen *et al.* [12] confirmed that glaucocalyxin A could inhibit the growth of human colorectal cancer cell (SW480), human hepatocellular carcinoma cell Bel-7402, human gastric cancer cell line SGC-7901 and human lymphoma HUT-78. The latest research has found that compounds from *I. suzhouensis* have good inhibitory activity on human prostatic cancer cell (LNCaP), human chronic myeloid leukemia cells (K562), lung cancer A549 and human cervical carcinoma hela, among which the compounds with α-methylene cyclopentanone structure have more significant

Received: September 13, 2024 Accepted: November 15, 2024

Meihui DUAN (1997-), female, P. R. China, master, devoted to research about chemistry and active components of natural medicines.

* Corresponding author. E-mail: nazi3647@sina.com.

anticancer activity[13].

At present, active components of antitumor effect of *I. suzhouensis* roots and its specific mechanism are not fully understood in the literature. Therefore, in this study, on the basis of UPLC-Q-TOF-MS analysis of chemical components of *I. suzhouensis* roots, combined with network pharmacology analysis, and preliminary verification by molecular docking, the material basis of the antitumor effect of *I. suzhouensis* roots and the possible molecular mechanism involved in regulation were systematically expounded, providing a scientific theoretical basis for further research and clinical treatment of the pharmacodynamic mechanism of *I. suzhouensis* roots.

## Materials and Methods

### Experimental materials

**Instruments** Liquid chromatography system: Dionex Ultimate 3000 RSLC (HPG) (Thermo Fisher Scientific); mass spectrometry system: Thermo Scientific Q Exactive Focus (Thermo Scientific Q Exactive Focus); ion source: HESI-II(Thermo Fisher Scientific); chromatographic column: ACE Ultracore 2.5 Super $C_{18}$, 100 mm × 2.1 mm (F-Bron).

**Medicinal materials and regents** Reagents: 95% ethanol; methanol (chromatographically pure); acetonitrile (chromatographically pure).

Medicinal materials: The medicinal materials were purchased from Bozhou medicinal materials market in Anhui Province and kept in the pharmaceutical laboratory of People's Hospital of Anshun City. They were identified by Han Zhengbin of Suzhou Luyuan Chinese Medicine Technology Co., Ltd. as *I. suzhouensis* of *Isodon* in Labiatae.

### Methods

**Analysis of chemical components in *I. suzhouensis* roots**

**Preparation of test solution** First, 50 mg of *I. suzhouensis* roots was extracted by refluxing with 10 times of 95% ethanol for 3 times, 3 h each time, and the extracts were combined. After filtration, the filtrate was concentrated under reduced pressure to recover ethanol and obtain a thick paste. Next, 10 mg of the sample was dissolved in 70% methanol water, and filtered through a 0.22 μm organic microporous filter membrane to obtain a sample solution of *I. suzhouensis* as the sample for LC-MS analysis.

**Chromatographic conditions** ACE Ultracore2.5 Super $C_{18}$ (100 mm × 2.1 mm); mobile phase: acetonitrile (0.1% formic acid)-0.1% formic acid water; gradient elution (0 – 2 min, 5% acetonitrile; 2 – 47 min, 95% acetonitrile; 47 – 50 min, 5% acetonitrile); volume flow rate: 0.3 ml/min; column temperature: 40 ℃.

**MS conditions** HESI-II ion source; ion source voltage: 3.0 kV (+)/2.5 kV (−); capillary heating temperature: 320 ℃; sheath gas flow rate: 35 arb; auxiliary gas flow rate: 10 arb; ion source temperature: 350 ℃; mass spectrometry scanning method: Full MS ddms2; scanning range: 100 – 1 500 m/z; primary resolution of Full MS: 70 000, and secondary resolution: 17 500.

**Network pharmacology analysis of *I. suzhouensis* roots**

**Screening of active components from *I. suzhouensis* roots and prediction of action targets** According to the UPLC-Q-TOF-MS analysis results of *I. suzhouensis* roots, the SMILES structure of identified compounds were obtained through the Pubchem database[14] (https://pubchem.ncbi.nlm.nih.gov/). Then, the SMILES structures or SDF format was input or uploaded into Swiss Target Prediction database[15] (http://swisstargetprediction.ch/), and after selecting "*Homo sapiens*" as the species, the information of compounds was predicted. The results were exported and saved in CSV format. Excel was employed to combine the targets of chemical components, and those with "probability ≥0" in the prediction results were selected. Next, the targets of potential active components were obtained after deleting duplicate items. Finally, the target proteins were transformed into standard gene names in the UniProt database[16] (https://www.uniprot.org/id-mapping/) and corrected.

**Collection of antitumor targets of *I. suzhouensis* roots** Through GeneCards database[17] (https://www.genecards.org), OMIM database (https://www.omim.org/) and Therapeutic Target Database (TTD) database (https://db.idrblab.net/ttd/), antitumor targets were searched using "inflammation" as the key word. Targets with relevance score ≥5 in the search results of GeneCards database were selected, and the target results screened by other databases were merged. Subsequently, antitumor targets were obtained after deleting duplicate items. Finally, intersecting targets of active component targets and antitumor targets were obtained using Venny 2.1.0 platform (https://bioinfogp.cnb.csic.es/tools/venny/index.html).

**Construction of protein interaction network (PPI) network and screening of core targets** According to the analysis by Venny 2.1.0, the intersecting targets were imported into the STRING database[18] (https://cn.string-db.org/), and protein interaction between the intersecting targets was predicted by selecting "Multiple proteins", "Homo sapiens" for species and highest confidence (0.900). The results of protein interaction were saved and downloaded in TSV file format. They were imported into Cytoscape 3.9.1 software for visualization. Network topology analysis was conducted using the Network Analyzer plug-in, and the Degree, Closeness and Betweenness values of targets were calculated. Intersecting targets with the three above the averages were selected as core targets, with degree as the parameter. A greater degree value meant that the node was more important.

**Gene ontology (GO) function and kyoto encyclopedia of genes and genomes (KEGG) pathway enrichment analysis** Through Metascape database[19] (http://metascape.org/gp/index.html#/main/step1), the intersecting targets of medicine activity and antitumor effect of *I. suzhouensis* roots were input. With *P* Value Cutoff = 0.01, the GO function enrichment analysis and KEGG pathway enrichment analysis were carried out, and the results were visualized. The molecular mechanism of the effective active components of *I. suzhouensis* roots in the treatment of tumor

diseases was further elaborated. Finally, diagrams were drawn by the bioinformatics platform (https://www.bioinformatics.com.cn/).

**Component-target-pathway network** An effective active component-antitumor target-pathway network diagram was constructed using Cytoscape 3.9.1 software, with nodes representing active components, intersecting targets and enrichment pathways, and edges representing their relationships. The Network Analyzer tool of the software was employed to calculate network topology characteristics, so as to screen core chemical components that exert antitumor effects.

**Molecular docking verification** According to the degree value, the top six core targets in PPI and the top six active components connected with the largest number of intersecting targets were selected for molecular docking verification in turn. The 3D structures of core target proteins were downloaded from PDB database[20] (https://www.rcsb.org/) in PDB format. PyMOL software was employed to delete water molecules and small molecular ligands, and the protein molecules were hydrogenated by AutoDock Tools 1.5.6 software, and finally saved in pdbqt format. Next, the Mol2 format files of active components were downloaded from TCMSP database[21] (https://old.tcmsp-e.com/tcmsp.php), or the SDF format files of 3D structures of active components were downloaded from PubChem database and converted into Mol2 format files with OpenBabel 3.1.1 software. The files were imported into AutoDock Tools 1.5.6 software to add atomic charges and assign atomic types. By default, all flexible bonds were rotatable and saved in pdbqt format. Molecular docking was carried out on active component and target proteins, and the results of molecular docking were visually analyzed by PyMOL software.

## Results and Analysis

### Main chemical components from *I. suzhouensis* roots

Samples were treated and detected according to the above methods using UPLC-Q-TOF-MS/MS technique. Based on MS information generated by chemical components in the ethanol extract of *I. suzhouensis* roots combined with secondary fragment ions, and according to references, the chemical components of *I. suzhouensis* roots were qualitatively analyzed. Finally, 59 compounds were identified from *I. suzhouensis* roots. Table 1 shows specific information of various chemical components.

**Table 1 Composition identification results of *I. suzhouensis* roots**

| No. | Compound name | Molecular formula | RT min | Detected ions | Ion fragments |
|---|---|---|---|---|---|
| 1 | Lactose | $C_{12}H_{22}O_{11}$ | 0.662 | $[M-H]^-$ | 341.107 94, 179.054 96, 119.033 64, 101.022 92, 89.022 91, 71.012 39, 59.012 41 |
| 2 | L-Valine | $C_5H_{11}NO_2$ | 0.766 | $[M+H]^+$ | 102.055 20, 82.065 65, 72.081 42, 59.073 70, 58.065 87 |
| 3 | Stachydrine | $C_7H_{13}NO_2$ | 0.829 | $[M+H-H_2O]^+$ | 98.096 54, 84.081 20, 72.081 39, 58.065 84 |
| 4 | L-Pyroglutamic acid | $C_5H_7NO_3$ | 1.068 | $[M+H]^+$ | 112.075 80, 84.044 97, 70.065 77, 56.050 22 |
| 5 | Matrine | $C_{15}H_{24}N_2O$ | 1.215 | $[M+H]^+$ | 218.152 80, 148.111 72, 110.096 61, 78.276 49 |
| 6 | Mannitol | $C_6H_{14}O_6$ | 1.216 | $[M-H]^-$ | 163.059 95, 119.033 64, 101.022 96, 89.022 95, 71.012 41, 59.012 43 |
| 7 | Ribitol | $C_5H_{12}O_5$ | 1.247 | $[M-H]^-$ | 131.033 20, 119.033 52, 101.022 93, 89.022 96, 71.012 40, 59.012 42, 55.017 50 |
| 8 | Orsellinic acid | $C_8H_8O_4$ | 1.448 | $[M-H]^-$ | 149.023 12, 139.038 65, 123.043 76, 109.028 10, 93.033 11, 67.017 50 |
| 9 | Danshensu | $C_9H_{10}O_5$ | 1.819 | $[M-H]^-$ | 179.033 78, 135.043 81, 123.043 77, 109.028 12, 95.048 79, 72.991 68 |
| 10 | Gentisic acid | $C_7H_6O_4$ | 2.204 | $[M-H]^-$ | 123.043 72, 109.028 05, 91.027 08, 81.033 10, 61.016 56 |
| 11 | 3,4-Dihydroxyphenylethanol | $C_8H_{10}O_3$ | 2.235 | $[M-H]^-$ | 135.043 72, 109.028 05, 108.020 20, 91.017 41, 81.033 17, 65.038 14 |
| 12 | 5-Hydroxymethylfurfural | $C_6H_6O_3$ | 2.439 | $[M+H]^+$ | 109.028 54, 95.049 55, 81.033 97, 53.039 33 |
| 13 | Protocatechualdehyde | $C_7H_6O_3$ | 3.398 | $[M-H]^-$ | 136.015 20, 119.012 24, 108.020 16, 93.033 309, 81.033 09, 65.038 15 |
| 14 | p-Hydroxybenzaldehyde | $C_7H_6O_2$ | 5.784 | $[M-H]^-$ | 109.012 70, 108.020 30, 93.033 16, 65.038 10 |
| 15 | Esculetin | $C_9H_6O_4$ | 5.994 | $[M-H]^-$ | 162.030 99, 149.023 16, 133.028 15, 105.033 13, 89.038 24, 81.033 04 |
| 16 | Caffeic acid | $C_9H_8O_4$ | 6.476 | $[M-H]^-$ | 135.043 84, 134.039 8, 107.048 68, 91.053 81, 79.053 79 |
| 17 | Ethyl gallate | $C_9H_{10}O_5$ | 6.738 | $[M+H]^+$ | 181.049 26, 153.054 29, 137.059 45, 125.059 60, 109.064 93, 97.065 18, 67.054 85 |
| 18 | Leucinic acid | $C_6H_{12}O_3$ | 6.84 | $[M-H]^-$ | 113.023 74, 102.987 47, 85.064 43, 71.012 44, 57.033 17 |
| 19 | 2-Hydroxy-4-methoxybenzaldehyde | $C_8H_8O_3$ | 8.514 | $[M+H]^+$ | 134.059 86, 125.059 61, 111.044 25, 93.033 82, 65.039 28 |
| 20 | Isovanillin | $C_8H_8O_3$ | 8.785 | $[M+H]^+$ | 125.059 65, 111.044 28, 93.033 185, 65.039 31 |

(Continued)

(Table 1)

| No. | Compound name | Molecular formula | RT min | Detected ions | Ion fragments |
|---|---|---|---|---|---|
| 21 | Vanillin | $C_8H_8O_3$ | 8.795 | $[M-H]^-$ | 136.015 23, 101.022 96, 89.022 95, 71.012 40, 59.012 42 |
| 22 | Puerarin | $C_{21}H_{20}O_9$ | 9.717 | $[M-H]^-$ | 295.060 52, 267.065 64, 223.075 38, 133.028 02, 105.033 11, 59.012 22 |
| 23 | 3,5-Dimethoxy-4-hydroxybenzaldehyde | $C_9H_{10}O_4$ | 10.271 | $[M+H]^+$ | 165.090 68, 155.069 93, 140.046 46, 123.044 02, 95.049 52, 67.054 86, 53.039 34 |
| 24 | Decursinol | $C_{14}H_{14}O_4$ | 10.38 | $[M+H]^+$ | 229.121 84, 211.111 31, 187.111 39, 159.116 44, 131.085 27, 105.070 06, 91.054 52, 68.997 67 |
| 25 | Arglabin | $C_{15}H_{18}O_3$ | 10.556 | $[M+H-H_2O]^+$ | 229.121 86, 211.111 27, 187.111 27, 159.116 49, 131.085 30, 105.070 05, 91.054 66, 68.997 76 |
| 26 | Suberic acid | $C_8H_{14}O_4$ | 10.732 | $[M-H]^-$ | 155.070 25, 129.090 71, 111.080 12, 83.048 75, 57.033 20 |
| 27 | 7-Methoxycoumarin | $C_{10}H_8O_3$ | 11.154 | $[M+H+MeOH]^+$ | 145.028 18, 134.036 01, 117.033 56, 89.038 99, 78.046 92 |
| 28 | Ferulic acid | $C_{10}H_{10}O_4$ | 11.163 | $[M+H]^+$ | 177.054 28, 145.028 17, 135.116 58, 117.033 55, 107.085 67, 89.038 99 |
| 29 | Dehydroandrographolide | $C_{20}H_{28}O_4$ | 12.007 | $[M+H]^+$ | 315.194 92, 263.163 94, 183.116 64, 95.085 82, 71.049 76 |
| 30 | Ethyl 3, 4-dihydroxybenzoate | $C_9H_{10}O_4$ | 13.261 | $[M-H]^-$ | 153.018 08, 137.059 949, 109.028 08, 89.022 99, 71.012 43, 59.012 46 |
| 31 | 3-Methoxy-4-hydroxyphenylacetate | $C_9H_{10}O_4$ | 13.813 | $[M-H]^-$ | 153.017 97, 137.059 48, 119.048 81, 107.048 80, 89.022 98, 71.012 40, 59.012 44 |
| 32 | Rosmarinic acid | $C_{18}H_{16}O_8$ | 13.94 | $[M-H]^-$ | 197.044 51, 179.033 91, 161.023 24, 133.028 17, 123.043 79, 72.991 70 |
| 33 | Agarotetrol | $C_{17}H_{18}O_6$ | 14.022 | $[M+H]^+$ | 301.214 87, 283.205 11, 185.095 86, 147.080 11, 105.070 07, 55.055 02 |
| 34 * | Dehydrodiisoeugenol | $C_{20}H_{22}O_4$ | 14.105 | $[M+H+MeOH]^+$ | 263.106 75, 175.075 30, 163.074 94, 137.059 45, 103.054 43, 91.054 45, 79.054 78 |
| 35 | Salvianolic acid C | $C_{26}H_{20}O_{10}$ | 15.819 | $[M-H]^-$ | 311.055 48, 267.065 64, 179.033 97, 135.043 82, 72.991 68 |
| 36 | Isosteviol | $C_{20}H_{30}O_3$ | 16.139 | $[M+H-H_2O]^+$ | 301.215 55, 233.152 97, 215.142 68, 187.147 63, 105.070 08, 69.070 51 |
| 37 | Ethyl caffeate | $C_{11}H_{12}O_4$ | 16.143 | $[M-H]^-$ | 179.033 81, 161.023 18, 135.043 81, 133.028 09 |
| 38 | Skimmin | $C_{15}H_{16}O_8$ | 16.935 | $[M+H-H_2O]^+$ | 163.038 68, 145.028 15, 135.043 82, 117.033 54, 89.038 90, 69.034 10 |
| 39 | Abietic Acid | $C_{20}H_{30}O_2$ | 17.372 | $[M+H]^+$ | 285.220 79, 243.174 01, 147.080 20, 133.064 59, 123.116 78, 81.070 31, 57.070 63 |
| 40 | Kurarinone | $C_{26}H_{30}O_6$ | 22.709 | $[M+H]^+$ | 397.198 09, 303.158 48, 197.044 08, 179.033 60, 151.038 64, 113.023 29, 95.049 39 |
| 41 * | Tetramethylcurcumin | $C_{25}H_{28}O_6$ | 25.145 | $[M-H]^-$ | 313.143 43, 261.148 90, 193.158 74, 161.023 10, 137.022 99, 124.015 17, 57.033 16 |
| 42 | Kahweol | $C_{20}H_{26}O_3$ | 25.491 | $[M+H]^+$ | 297.184 54, 269.189 36, 227.142 38, 175.111 39, 133.064 56, 95.085 82 |
| 43 | Medicagenic acid | $C_{30}H_{46}O_6$ | 25.723 | $[M-H]^-$ | 483.309 75, 439.320 80, 423.289 73, 413.339 97, 379.298 58, 189.127 14 |
| 44 | Methyl hexadecanoate | $C_{17}H_{34}O_2$ | 26.423 | $[M-H]^-$ | 297.242 68, 279.232 91, 201.112 03, 171.101 44, 141.127 15, 127.114 0 |
| 45 | Ginkgolic acid C17-1 | $C_{24}H_{38}O_3$ | 26.439 | $[M+H]^+$ | 287.236 08, 231.210 07, 135.080 17, 109.101 30, 95.085 85, 69.070 51 |
| 46 * | Isosteviol | $C_{20}H_{30}O_3$ | 26.624 | $[M+H]^+$ | 301.215 88, 273.220 73, 255.209 99, 165.127 17, 151.111 54, 121.101 14, 94.070 27 |
| 47 | α-Linolenic acid | $C_{18}H_{30}O_2$ | 28.119 | $[M+H]^+$ | 137.132 39, 123.116 76, 109.101 36, 95.085 88, 81.070 40, 67.054 92 |
| 48 * | Ursonic acid | $C_{30}H_{46}O_3$ | 28.55 | $[M+H]^+$ | 437.341 40, 409.345 31, 203.179 11, 189.163 38, 119.085 55, 95.085 85 |
| 49 * | Echinocystic acid | $C_{30}H_{48}O_4$ | 28.692 | $[M-H]^-$ | 407.331 88, 214.366 10, 98.030 89, 58.004 65 |

(Continued)

(Table 1)

| No. | Compound name | Molecular formula | RT min | Detected ions | Ion fragments |
|---|---|---|---|---|---|
| 50 * | Oleanonic acid | $C_{30}H_{46}O_3$ | 30.717 | $[M+H]^+$ | 409.346 95, 259.168 85, 189.163 35, 119.085 58, 95.085 84, 69.070 45 |
| 51 | Maslinic acid | $C_{30}H_{48}O_4$ | 31.109 | $[M+H]^+$ | 427.356 32, 357.278 44, 201.163 50, 69.070 53 |
| 52 | Bryodulcosigenin | $C_{30}H_{50}O_4$ | 31.871 | $[M+H]^+$ | 437.34174, 287.199 83, 189.163 41, 133.101 06, 119.085 48, 107.085 73, 95.085 87, 81.070 46 |
| 53 | Abietic Acid | $C_{20}H_{30}O_2$ | 32.919 | $[2M+Na]^+$ | 285.220 67, 257.225 77, 201.163 50, 149.132 25, 109.101 24, 95.085 84, 81.070 40, 67.054 89, 55.054 99 |
| 54 | Acetyl-11-keto-β-boswellic acid | $C_{32}H_{48}O_5$ | 33.011 | $[M+H]^+$ | 467.348 85, 407.333 13, 317.210 63, 189.163 39, 119.085 55, 95.085 83 |
| 55 | 3-O-Acetyl-1α-hydroxytrametenolic acid | $C_{32}H_{50}O_5$ | 36.371 | $[M+H]^+$ | 469.366 76, 373.272 40, 301.213 53, 189.163 18, 119.085 59, 107.085 66, 81.070 33 |
| 56 | Lupenone | $C_{30}H_{48}O$ | 36.378 | $[M+H]^+$ | 217.194 53, 191.171 899, 149.132 14, 95.085 83, 81.070 38 |
| 57 | Flavanone | $C_{15}H_{12}O_2$ | 37.78 | $[M-H]^-$ | 206.995 85, 149.008 19, 92.999 86, 74.989 30, 59.965 69 |
| 58 | D-Glyceric acid | $C_3H_6O_4$ | 40.453 | $[M-H]^-$ | 149.008 26, 137.023 13, 109.028 27, 92.999 86, 74.989 27, 59.966 01 |

* indicates the top six key active components.

**Network pharmacology analysis of *I. suzhouensis* roots**

**Screening of active components from *I. suzhouensis* roots and prediction of action targets** Targets of 58 compounds were predicted using Swiss Target Prediction database. No targets were found for 3,4-dihydroxyphenylethanol, decursinol and agarotetrol, and a total of 55 potential active components of *I. suzhouensis* roots were predicted. After being corrected into standard gene names in UniProt database, 716 potential targets were obtained after de-duplication.

**Analysis on potential antitumor targets of *I. suzhouensis* roots**

According to the screening method in "Collection of antitumor targets of *I. suzhouensis* roots", 976 targets were screened in GeneCards database, and 14 targets were screened in OMIM database, and 986 antitumor targets were obtained in TTD database. Then, a Venn diagram was drawn between the predicted targets of active components and the target genes of diseases. Finally, 202 intersecting targets were obtained as potential targets for the antitumor effect of *I. suzhouensis* roots, as shown in Fig. 1.

**PPI network and core targets** First, 202 intersecting targets obtained by Venny 2.1.0 analysis were uploaded to STRING database, and a PPI network was constructed. Finally, the PPI network model with 38 target protein nodes and 625 edges was obtained. The PPI network diagram is shown in Fig. 2. Meanwhile, the file in TSV format was download and saved, and imported into Cytoscape 3.9.1 software for visualization. Network topology analysis was conducted using the Network Analyzer plug-in, and 38 core targets were obtained with the conditions of Degree >45.455 4, closeness >0.004 946 and betweenness >167.996 from the data screened with Degree as the parameter. These core targets were sorted in descending order as following: serine/threonine protein kinase 1 (AKT1), tumor protein p53 (TP53), albumin (ALB), glyceraldehyde-3-phosphate dehydrogenase (GAPDH), cadherin-related protein (CTNNB1), sarcoma virus protein (SRC), epidermal growth factor receptor (EGFR), tumor necrosis factor (TNF), interleukin-6 (IL6), vascular endothelial growth factor A (VEGFA), JUN (transcription factor AP-1), signal transducer and activator of transcription 3 (STAT3), cysteinyl aspartate specific proteinase 3 (CASP3), recombinant mitogen activated protein kinase 3 (MAPK3), 90kDa heat shock protein AA1 (HSP90AA1), estrogen receptor 1 (ESR1), rapamycin (MTOR), cyclin D1 (CCND1), tyrosine kinase receptor 2 (ERBB2), peroxisome proliferators-activated receptor (PPARG), extracellular protein regulated kinase 1 (MAPK1), sirtuin 1 (SIRT1), cyclooxygenase 2 (PTGS2), matrix metalloproteinase (MMP9), PIK3CA, MDM2, EP300, V-Rel reticuloendotheliosis viral oncogene homolog A (RELA), toll-like receptor 4 (TLR4), mitogen-activated protein kinase 14 (MAPK14), interleukin 2 (IL-2), endothelial nitric oxide synthase (NOS3), androgen receptor (AR), peroxisome proliferators-activated receptor A (PPARA), PGR, glucocorticoid receptor gene (NR3C1), angiotensin converting enzyme (ACE), and renin (REN). These results indicated that these targets were of great significance to the antitumor effect of *I. suzhouensis* roots.

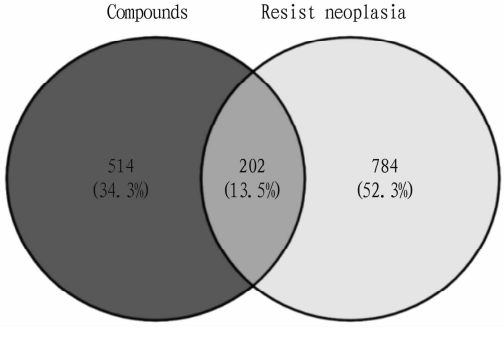


**Fig. 1 Venn diagram of drug targets and antitumor targets**

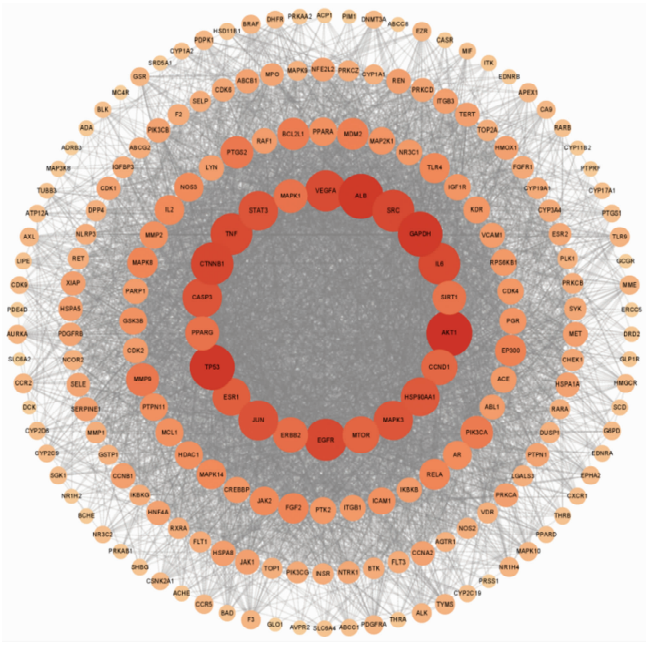

**Fig. 2 Visual antitumor PPI network diagram of *I. suzhouensis* roots**

## GO function and KEGG pathway enrichment analysis

Metascape database was used to analyze the GO function enrichment and KEGG pathway enrichment of antitumor targets of *I. suzhouensis* roots, and the results were visualized. GO function enrichment analysis showed that 2 591 GO biological function items were obtained. Among them, 2 245 items were related to biological process (BP), mainly including the response to hormones, phosphorylation, cellular response to lipid, response to xenbiotic stimulus, positive regulation of phosphorus metabolism process, response to nutritional level, positive regulation of cell migration, cellular response to chemical stress, cellular response to organic cyclic compound, and regulation of apoptosis signal pathway. There were 117 items related to cell component (CC), mainly including receptor complex, membrane raft, membrane microdomain, perinuclear region of cytoplasm, side of membrane, protein kinase complex, focal adhesion, cell-substrate junction, transferase complex, transferring phosphorus-containing group, and neuronal cell body. And 229 items related to molecular function (MF), mainly involving protein kinase activity, phosphotransferase activity, alcohol group as receptor, kinase activity, protein kinase binding, protein tyrosine kinase activity, kinase binding, protein serine/threonine kinase activity, protein serine kinase activity, transcription factor binding, and nuclear receptor activity. According to the P value, the top 10 items of BP, CC and MF enrichment genes were selected to draw a bar chart, and the results are shown in Fig. 3. The results of KEGG pathway enrichment analysis showed that 201 antitumor signal pathways were obtained for *I. suzhouensis* roots, mainly including pathways in cancer, PI3K-Akt, lipid and atherosclerosis, prostate cancer, proteoglycans in cancer, AGE-RAGE, EGFR tyrosine kinase inhibitor resistance, KSHV, kaposi sarcoma-associated herpesvirus infection, endocrine resistance, fluid shear stress and atherosclerosis, pancreatic cancer, hepatitis B, MAPK, human cytomegalovirus infection, FoxO, chemical carcinogenesis-receptor activation, focal adhesion, MicroRNAs in cancer, HIF-1, and insulin resistance. The above-mentioned pathways were screened by the condition of P value and a large number of enriched genes, and the top 20 pathways were selected to draw a bubble diagram, as shown in Fig. 4.

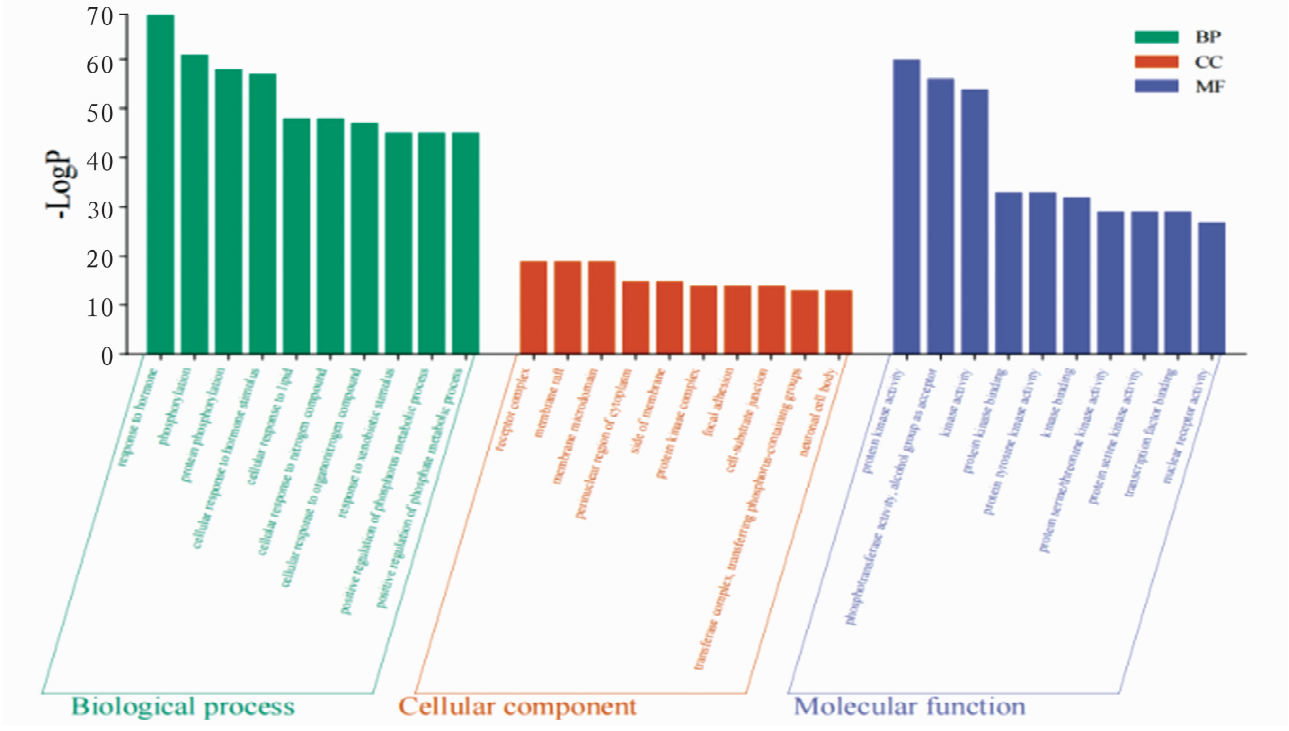

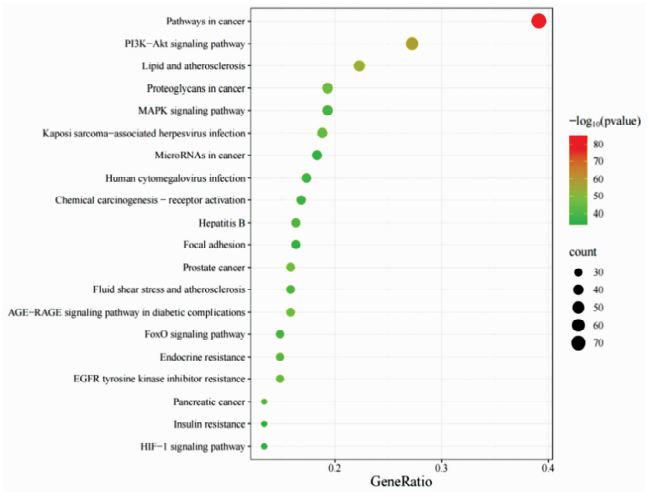


**Fig. 4 Enrichment analytic diagram of KEGG pathway**

**Component-target-pathway network** The antitumor active components of *I. suzhouensis* roots were associated with the top 20 signal pathways and their enriched target genes, and the network diagram of "active component-antitumor target-enrichment pathway" was constructed by using Cytoscape 3.9.1 software, as shown in Fig. 5. The network consists of 276 nodes (52 active component nodes, 202 inflammatory target nodes and 20 pathway nodes) and 1 677 edges. According to the network topology parameter, the degree value, the top six active components were screened out as following: dehydrodiisoeugenol, tetramethylcurcumin, isosteviol, ursonic acid, echinocystic acid and oleanonic acid, indicating that these components play a key role in the antitumor process.

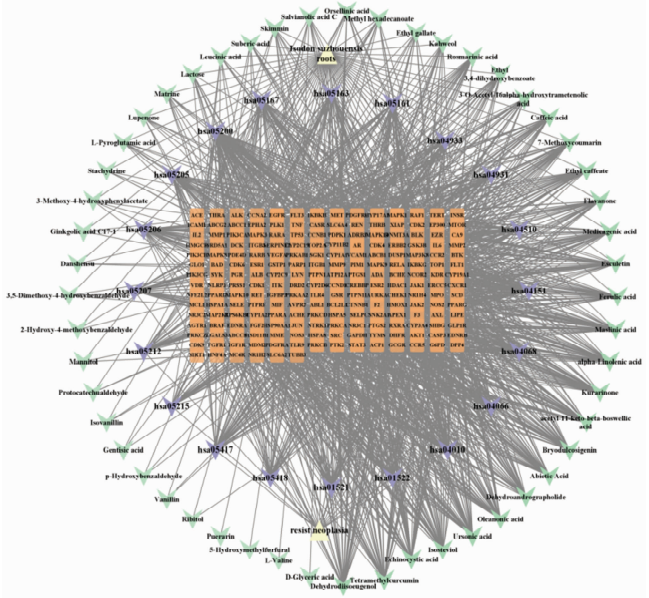


Yellow in the diagram represents the herb and disease; green represents active components; purple represents pathways; and orange stands for gene targets.

**Fig. 5 Component-target-pathway network diagram**

**Molecular docking verification** The top six core targets in PPI and the top six active components in terms of degree value in the "component-target-pathway" network were verified by molecular docking using AutoDock Tools 1.5.6 software, and the results are shown in Table 2. It is generally believed that the lower the binding energy of molecular docking, the higher the binding affinity. When the binding energy is $\leqslant -4.25$ kcal/mol, it indicates that there is certain binding activity between the active component and the target. A binding energy $\leqslant -5.0$ kcal/mol indicates that the active component and the target have good binding activity. A binding energy $\leqslant -7.0$ kcal/mol indicates that they have strong binding activity[22]. The results of molecular docking showed that two groups showed certain binding activity, and seven groups showed good binding activity, and most of them showed strong binding activity, indicating that the above components acting on these targets might be the potential mechanism of the antitumor effect of *I. suzhouensis* roots. PyMOL software was used for visual analysis, as shown in Fig. 6. The visualization results showed that the active components mainly formed hydrogen bonds at nine hydrophilic amino acid residue binding sites: glutamine (GLN), asparagine (ASN), threonine (THR), lysine (LYS), glutamic acid (GLU), glycine (GLY), tyrosine (TYR), cysteine (CYS) and serine (SER), and they form hydrophobic interaction with five

**Table 2 Binding energy of active components and core targets**

| Compound | Binding energy//kcal/mol | | | | | |
|---|---|---|---|---|---|---|
| | AKT1 | TP53 | ALB | GAPDH | CTNNB1 | SRC |
| Tetramethylcurcumin | −7.41 | −5.69 | −5.01 | −4.93 | −4.40 | −9.60 |
| Isosteviol | −7.84 | −7.64 | −8.07 | −8.86 | −7.62 | −9.25 |
| Ursonic acid | −7.78 | −8.15 | −7.19 | −8.97 | −6.91 | −10.04 |
| Oleanonic acid | −8.86 | −8.36 | −7.10 | −8.72 | −7.14 | −10.51 |
| Dehydrodiisoeugenol | −6.65 | −6.75 | −7.60 | −7.34 | −5.97 | −8.52 |
| Echinocystic acid | −8.53 | −7.29 | −6.80 | −7.96 | −7.79 | −8.89 |

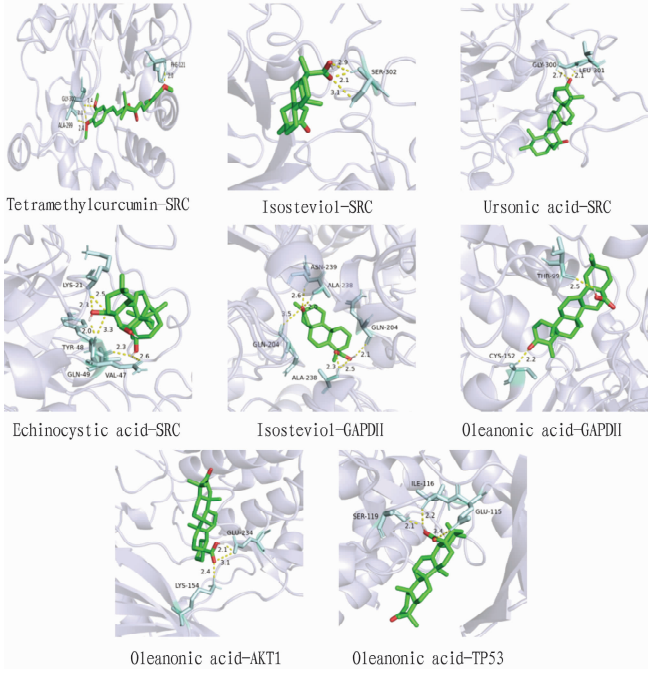


**Fig. 6 Diagrams of molecular docking**

hydrophobic amino acids, valine (VAL), leucine (LEU), alanine (ALA), phenylalanine (PHE) and isoleucine (ILE). Among them, tetramethylpcurcumin formed hydrogen-bond interaction at amino acid residue GLY (glycine)-300 in SRC protein, and hydrophobic effects with ALA (alanine)-299 and PHE (phenylalanine)-121. Isosteviol formed hydrogen-bond interaction at amino acid residues SER (serine)-302 in SRC protein and at ASN (asparagine)-239 and GLN (glutamine)-204 in GAPDH protein respectively, and hydrophobic effect with ALA (alanine)-238. Ursonic acid formed hydrogen-bond interaction at amino acid residue GLY (glycine)-300 in SRC protein, and hydrophobic effect with LEU (leucine)-301. Echinocystic acid formed hydrogen-bond interaction at LYS (lysine)-21, TYR (tyrosine)-48 and GLN (glutamine)-49 in SRC protein respectively, and formed hydrophobic effect with VAL (valine)-47. Oleanonic acid formed hydrogen-bond interaction at amino acid residues THR (threonine)-99 and CYS (cysteine)-152 in GAPDH protein, at amino acid residues GLU (glutamic acid)-234 and LYS (lysine)-154 in AKT1 protein, and at amino acid residues SER (serine)-119 and GLU (glutamic acid)-153 in TP53 protein, respectively, and it formed hydrophobic effect with ILE (isoleucine)-116.

## Discussion

In this study, 55 effective active components of *I. suzhouensis* roots and 716 antitumor target genes were screened out by UPLC-Q-TOF-MS/MS technique combined with network pharmacology, and 202 potential antitumor targets of *I. suzhouensis* roots were obtained by intersecting the 716 antitumor target genes with 986 cancer target genes screened by disease database. The PPI network of the 202 protein targets was constructed by STRING database, and 38 core targets including AKT1, TP53, ALB, GAPDH, CTNNB1 and SRC were screened out. Related studies showed that piperine, as a new active component in the treatment of prostate cancer, has certain toxicity. Through MD simulation, it was found that piperine-akt1 complex has high stability in the treatment of prostate cancer by binding with hydrophilic residues Lys268 and Ser205[23]. Traditional Chinese medicine regulates TP53 to achieve the effects of regulating apoptosis, blocking cell cycle, preventing angiogenesis, regulating metabolism and autophagy, promoting pyroptosis and ferroptosis, and affecting immune response[24]. Serum ALB is significantly related to the therapeutic effect and prognosis of lung cancer patients[25]. Viral cancer (SRC) gene is the first oncogene with intrinsic tyrosine kinase activity, and this protein can be used as various downstream signal pathways such as growth factors mediated by non-receptor tyrosine kinases, thus inhibiting the growth of cancer cells[26].

KEGG pathway enrichment analysis showed that the antitumor targets of *I. suzhouensis* roots were mainly enriched in signaling pathways such as pathways in cancer, PI3K Akt, lipid and atherosclerosis, prostate cancer, proteoglycans in cancer, and AGE-RAGE[27]. Antitumor angiogenesis can be achieved by regulating TP53 and other targets to act on AGE-RAGE, IL-17, FSS and other pathways, thus playing an antitumor role[24,28]. It can be seen that multiple signal pathways may participate in the development of cancer in a synergistic way.

The active components related to cancer treatment from *I. suzhouensis* roots were screened by component-target-pathway network analysis, mainly including dehydrodiisoeugenol, tetramethylcurcumin, isosteviol, ursonic acid, echinocystic acid and oleanonic acid. Related studies show that isosteviol and its derivatives have good antitumor activity on HCT116, Huh7 and SW620 cells[29]. Curcumin can inhibit the expression of matrix metalloproteinases and vascular endothelial growth factor, block the blood supply, and then realize the apoptosis of tumor cells. In addition, it can enhance the immune function of rats[30]. Dehydrodiisoeugenol can inhibit the proliferation of colon cancer by blocking the cell cycle, and it can also induce endoplasmic reticulum stress-related autophagy of the autophagy flow blocking type, which inhibits the growth of colon cancer cells and exhibits excellent anti-colon cancer activity at the cellular and individual water levels[31]. Xia *et al.*[32] found that diterpenoids from *I. suzhouensis* could influence and regulate caspase-3, caspase-9 and Bax, leading to the apoptosis of SiHa cells. Based on this, the active components of *I. suzhouensis* roots were molecularly docked with the core targets. The results showed that all of them had certain binding activity, and most of them showed strong binding activity. It could be seen that after entering the body, the active components of *I. suzhouensis* roots might synergistically act on multiple protein targets and signaling pathways in the form of multiple components to exert antitumor effects.

To sum up, *I. suzhouensis* roots might play an antitumor role through core components such as dehydrodiisoeugenol, tetramethylcurcumin, isosteviol, ursonic acid, echinocystic acid and oleanonic acid, which acted on AKT1, TP53, ALB, GAPDH, CTNNB1, SRC and other core targets, which regulated pathways such as pathways in cancer, PI3K-Akt, lipid and atherosclerosis, prostate cancer, proteoglycans in cancer and AGE-RAGE, and biological processes such as the response to hormones, phosphorylation, cellular response to lipid, response to xenbiotic stimulus, positive regulation of phosphorus metabolism process, and response to nutritional level. This conclusion provides a scientific and reasonable theoretical basis for further study on the material basis and mechanism of antitumor effect of *I. suzhouensis* roots.

## *References*

[1] HAN B, ZHENG R, ZENG H, *et al.* Cancer incidence and mortality in China, 2022[J]. J Natl Cancer Cent., 2024, 4(1): 47-53.

[2] CUI J, SHI WW, SU Y, *et al.* Studies on triterpenoids from *Isodon suzhouensis*[J]. Journal of Anhui University of Chinese Medicine, 2011, 30(3): 57-59. (in Chinese).

[3] WEI JT. Study on the anti-tumor effect and mechanism of oleanolic acid [D]. Graduate School of China Academy of Sciences (Oceanography Institute), 2012. (in Chinese).

[4] ZHANG XH. Clinical application of antibacterial effect of Chinese herbal medicine *Rabdosia amethystoides* (Benth.)[J]. Clinical Medicine of China, 1982(5): 13-14, 66. (in Chinese).

[5] CORLAY N, LECSÖ-BORNET M, LEBORGNE E, *et al.* Antibacterial labdane diterpenoids from *Vitex vestita*[J]. J Nat Prod., 2015, 78(6): 1348-1356.

[6] WANG YC, WANG M, ZHAI KF, *et al.* Study on purification technique

of total terpenoids in the roots of *Isodon suzhouensis* [J]. Journal of Huanghe S&T College, 2020, 22(8): 11 – 15. (in Chinese).
[7] TIAN T, CHEN H, ZHAO Y. Traditional uses, phytochemistry, pharmacology, toxicology and quality control of Alisma orientale (Sam.) Juzep: A review[J]. Journal of Ethnopharmacology. 2014, 158(A): 373 – 387.
[8] YAO S, CHU CJ, HAN HY, *et al.* Study on antithrombotic effect of glaucocalyxin[J]. Journal of Liaoning University of Traditional Chinese Medicine, 2012(11): 61 – 65. (in Chinese).
[9] DING L, HOU Q, ZHOU Q, *et al.* Structure-activity relationships of eight ent-kaurene diterpenoids from three *Isodon* plants[J]. Research On Chemical Intermediates, 2010, 36(4): 443 – 452.
[10] GAN P, ZHANG L, CHEN Y, *et al.* Anti-inflammatory effects of glaucocalyxin B in microglia cells[J]. Journal of Pharmacological Sciences, 2015, 128(1): 35 – 46.
[11] KIM BW, KOPPULA S, HONG SS, *et al.* Regulation of microglia activity by glaucocalyxin-A: Attenuation of lipopolysaccharide-stimulated neuroinflammation through NF-kappaB and p38 MAPK signaling pathways [J]. PLoS One. 2013, 8(2): e55792.
[12] SHEN XD, CAO L, DONG X, *et al.* Study on the cytotoxic effect of glaucocalyxin A *in vitro* [J]. Chinese Archives of Traditional Chinese Medicine, 2011, 29(6): 1334 – 1335. (in Chinese).
[13] WEI MQ, CHEN L, ZHANG WQ, *et al.* Study on chemical components and antitumor activity of *Isodon suzhouensis*[J/OL]. Natural Product Research and Development 1 – 16[2024 – 10 – 22]. http://kns.cnki.net/kcms/detail/51.1335.Q.20241011.1835.005.html. (in Chinese).
[14] BOLTON E, CHEN J, KIM S, *et al.* PubChem3D: a new resource for scientists[J]. Journal of cheminformatics, 2011, 3: 1 – 15.
[15] DAINA A, MICHIELIN O, ZOETE V. SwissTargetPrediction: updated data and new features for efficient prediction of protein targets of small molecules[J]. Nucleic acids research, 2019, 47(W1): W357 – W364.
[16] UniProt: the Universal Protein knowledgebase in 2023 [J]. Nucleic Acids Research, 2023, 51(D1): D523 – D531.
[17] STELZER G, ROSEN N, PLASCHKES I, *et al.* The GeneCards suite: From gene data mining to disease genome sequence analyses[J]. Curr Protoc Bioinformatics, 2016, 54: 1.30.1 – 1.30.33.
[18] SZKLARCZYK D, GABLE AL, NASTOU KC, *et al.* The STRING database in 2021: Customizable protein-protein networks, and functional characterization of user-uploaded gene/measurement sets [J]. Nucleic acids research, 2021, 49(D1): D605 – D612.
[19] ZHOU Y, ZHOU B, PACHE L, *et al.* Metascape provides a biologist-oriented resource for the analysis of systems-level datasets[J]. Nature communications, 2019, 10(1): 1523.
[20] SEHNAL D, BITTRICH S, DESHPANDE M, *et al.* Mol * Viewer: Modern web app for 3D visualization and analysis of large biomolecular structures[J]. Nucleic Acids Research, 2021, 49(W1): W431 – W437.
[21] RU J, LI P, WANG J, *et al.* TCMSP: A database of systems pharmacology for drug discovery from herbal medicines [J]. Journal of cheminformatics, 2014, 6: 1 – 6.
[22] WEI MQ, ZHANG WQ, LIANG W, *et al.* Study on anti-inflammatory substances and mechanism of *Isodon suzhouensis* leaves based on UPLC-Q-TOF-MS/MS, network pharmacology and molecular docking [J]. Guizhou Science, 2024, 42(2): 23 – 33. (in Chinese).
[23] NAYANA P, GOLLAPALLI P, MANJUNATHA H. Investigating the structural basis of piperine targeting AKT1 against prostate cancer through *in vitro* and molecular dynamics simulations[J]. J Biomol Struct Dyn., 2024, 26: 1 – 15.
[24] LI JK, WANG LJ, SI WT. Study on the mechanism of TCM Regulating TP53 for resisting tumor[J/OL]. Acta Chinese Medicine, 1 – 10[2024 – 10 – 25]. http://kns.cnki.net/kcms/detail/41.1411.R.20240808.1328.026.html. (in Chinese).
[25] LI X, MAO Y, WANG LF, *et al.* Study on the relationship between serum PNI, LMR, ALB/GLB and treatment efficacy and prognosis of elderly patients with non-small cell lung cancer[J]. Progress in Modern Biomedicine, 2024, 24(14): 2699 – 2703, 2718. (in Chinese).
[26] SRIDARAN D, CHOUHAN S, MAHAJAN K, *et al.* Inhibiting ACK1-mediated phosphorylation of C-terminal Src kinase counteracts prostate cancer immune checkpoint blockade resistance[J]. Nat Commun, 2022, 13(1): 6929.
[27] SU XX, HAN L, LUO WZ, *et al.* The anti-tumor effect of Xuanfuhua decoction combined with sorafenib on liver cancer bearing mice based on PTEN/PI3K/AKT signaling pathway[J]. Chinese Pharmacological Bulletin, 2024, 40(10): 1884 – 1892. (in Chinese).
[28] XU J, CHEN L, YU J, *et al.* Involvement of advanced glycation end products in the pathogenesis of diabetic retinopathy[J]. Cellular Physiology and Biochemistry, 2018, 48(2): 705 – 717.
[29] LIU Y, WANG TT, CHEN L. Synthesis and antitumor activity of isosteviol derivatives[J]. Journal of China Pharmaceutical University, 2016, 47(1): 48 – 53. (in Chinese).
[30] CHEN HM, FENG Q, LI J, *et al.* Effects of curcumin on apoptosis and immune function of tumor cells in cervical cancer rats and its mechanism [J]. Chinese Journal of Gerontology, 2023, 43(13): 3271 – 3274. (in Chinese).
[31] LI CH. Study on the anti-colon cancer effect and mechanism of dehydrodiisoeugenol[D]. Chongqing: Southwest University, 2021. (in Chinese).
[32] XIA W, WANG X, JIANG X, *et al.* The inhibitory effect of glaucocalyxin A on human cervical carcinoma SiHa cells[J]. Chinese Pharmacological Bulletin. 2011, 27: 1035 – 1036.

Editor: Yingzhi GUANG Proofreader: Xinxiu ZHU

# Correction Statement

The article titled "Effects of Astragalus membranaceus on Energy Metabolism and Expression of CNTF Protein in Skeletal Muscle of Exercise-induced Fatigue Rats", which was published in Volume 12, No. 6, 2023, pp. 19-24,29, is hereby corrected due to an error in the grant number of a fund. The corrected funds are as follows:

Supported by Undergraduate Innovation and Entrepreneurship Training Program of Guizhou University of Traditional Chinese Medicine (GZYDCHZ [2019] 22); National Key R&D Plan (2019YFC1712500); Guizhou Provincial Science and Technology Planning Project (QKHHBZ [2020] 3003).

Other contents of the article remain unchanged, which is hereby explained.